Contents lists available at SciOpen

Food Science and Human Wellness

journal homepage: https://www.sciopen.com/journal/2097-0765

China Food Publishing Co.

Unveiling the safe dose range of the conjugated linolenic acid *cis*9,*trans*11,*cis*15-CLNA from *Bifidobacterium breve*

Zihuan Wu[a,b], Haiqin Chen[a,b,*], Bo Yang[a,b], Jianxin Zhao[a,b,c], Wei Chen[a,b]

[a] *State Key Laboratory of Food Science and Resources, Jiangnan University, Wuxi 214122, China*
[b] *School of Food Science and Technology, Jiangnan University, Wuxi 214122, China*
[c] *National Engineering Research Center for Functional Food, Jiangnan University, Wuxi 214122, China*

ARTICLE INFO

Article history:
Received 27 July 2024
Received in revised form 24 August 2024
Accepted 23 September 2024

Keywords:
*cis*9,*trans*11,*cis*15-CLNA
Acute toxicity
Subchronic toxicity
Peroxisome proliferator-activated receptor gamma

ABSTRACT

Previous studies have demonstrated that *cis*9,*trans*11,*cis*15-CLNA (c9,t11,c15-CLNA), a metabolite of *Bifidobacterium breve* CCFM683, possesses anti-inflammatory properties in the intestine. However, its safety profile remains unexplored. This study establishes the safe dose range for c9,t11,c15-CLNA and investigates the potential damage pathways. The results indicate that the maximum safe dose for mice is lower than 625 mg/kg, primarily due to hepatocyte damage. In cellular experiments revealed that an overdose of c9,t11,c15-CLNA activates peroxisome proliferator-activated receptor gamma (PPAR-γ), leading to hepatic lipid accumulation. The addition of the PPAR-γ inhibitor partially mitigated this effect. In summary, this study established that the maximum tolerated dose of c9,t11,c15-CLNA in healthy adult C57BL/6N mice is 625 mg/kg. For human application, the estimated safe dose is below 50.62 mg/kg. Additionally, c9,t11,c15-CLNA was found to activate the PPAR-γ protein in the liver, leading to lipid accumulation within hepatic tissue.

1. Introduction

Fatty acids, as an important and indispensable part of the diet, play a vital role in human growth and development, energy supply, and physiological metabolism[1]. Among them, EPA and DHA are 2 fatty acids that can lower blood triglyceride levels and reduce the risk of cardiovascular disease[2]. Conjugated linolenic acids (CLNAs) are a newly discovered class of polyunsaturated fatty acids with a special structure in which the carbon-carbon double bonds are arranged in a conjugated manner[3-4]. Recent studies have shown that CLNAs not only have antioxidant, anti-inflammatory, and energy metabolism regulating effects but also may have potential benefits in preventing metabolic diseases such as obesity, diabetes, and cancer[3-4]. This makes CLNAs promising candidates for the development of health foods and food additives, an area of increasing scientific interest[3-4].

CLNAs were initially discovered and isolated from certain plant seed oils, such as perilla seed oil and blue rhamnus seed oil. Their main isomers include α-eleostearic acid (*cis*9,*trans*11,*trans*13-18:3), calendic acid (*trans*8,*trans*10,*cis*12-18:3), and catalpic acid (*cis*9,*trans*11,*cis*13-18:3). Recent research has shown that microorganisms can also generate CLNAs through metabolic pathways. In our previous study, we found that CLNAs were produced by different mechanisms in strains such as *Lactobacillus plantarum* ZS2058 and *Bifidobacterium breve* CCFM683. This study focuses on the conjugated linolenic acid produced by *B. breve* CCFM683[5-6]. Previous studies inferred its structure to be *cis*9,*trans*11,*cis*15-CLNA

* Corresponding author at: State Key Laboratory of Food Science and Resources, Jiangnan University, Wuxi 214122, China.
E-mail address: haiqinchen@jiangnan.edu.cn (H.Q. Chen)
Peer review under responsibility of Beijing Academy of Food Sciences.

SciOpen Publishing services by Tsinghua University Press

http://doi.org/10.26599/FSHW.2024.9250444

(c9,t11,c15-CLNA) based on enzymatic catalytic characteristics and reported that it could alleviate dextran sulfate sodium (DSS)-induced colitis in mice at a dose of 400 μg/day, with effects superior to those of punicic acid (PA)[7]. *In vitro* studies demonstrated that 20 μmol/L of c9,t11,c15-CLNA could effectively inhibit the proliferation of colon cancer cells Caco-2, SW480, and HT-29[8]. Its analogs *cis*9,*trans*11,*cis*13-CLNA and *cis*9,*trans*11,*trans*13-CLNA also exhibited anti-oxidation and immune enhancement effects[4]. Consequently, the c9,t11,c15-CLNA exhibits promising potential for addition into postbiotic formulations or other functional food products. Regrettably, a structurally analogous compound, pomegranate seed oil (rich in *cis*9,*trans*11,*cis*13-CLNA), has been demonstrated to impair high-density lipoprotein levels when consumed daily at a dose of 0.15 mL over an extended period[3]. Another isomer, *cis*9,*cis*12,*cis*15-conjugated linolenic acid, has been identified in *Moringa oleifera*, exhibiting cardiovascular protective and neuroprotective properties[9]. However, excessive intake may lead to skin allergies and hepatotoxicity. Therefore, if the safe dosage range for octadecatrienoic acids cannot be clearly defined, it will significantly limit their application in food products. Consequently, this study aims to thoroughly evaluate the appropriate dosage range for c9,t11,c15-CLNA, laying the groundwork for its subsequent research and development in food applications.

The primary of this paper is to investigate the safe dosage range for c9,t11,c15-CLNA, along with its potential adverse effects and mechanisms. We will conduct safety dose experiments focusing on assessing acute and subchronic toxicity experiments. Acute toxicity is primarily evaluated by determining the median lethal dose (LD_{50}), whereas subchronic toxicity is assessed through organ coefficients, hematological indices, biochemical indices, and histological examinations. Furthermore, we will examine potential mechanisms underlying adverse reactions by focusing on affected organs and target proteins of c9,t11,c15-CLNA analogs. Specifically, we will explore whether c9,t11,c15-CLNA activates peroxisome proliferator-activated receptor gamma (PPAR-γ) and whether excessive activation is the primary cause of harm. Our goal is to gather data on the safe dosage of c9,t11,c15-CLNA and comprehend the mechanism of harm after an overdose for its in-depth development. This study will also establish a robust foundation for the future development and application of c9,t11,c15-CLNA in food products or other areas.

2. Materials and methods

2.1 Acquisition of c9,t11,c15-CLNA

The source, preparation, and characterization of c9,t11,c15-CLNA were based on Ren's article[7]. The procedure involved activating the CCFM683 strain using modified de Man, Rogosa and Sharpe medium (mMRS) plate medium followed by inoculation in liquid mMRS for incubation. After 18 h, the bacterial solution was introduced into 4 L of mMRS medium with an inoculum volume of 2% and a final substrate concentration of 0.5 mg/mL. The fermentation lasted for 24 h before being halted. The extraction process involved a mixture of fermentation broth, isopropanol, and hexane in a 1:1:2 ratio. The *n*-hexane layer was collected and dried by spin evaporation before undergoing liquid phase purification to yield purified oils. The purified fats were tested for purity using gas chromatography-mass spectrometry (GC-MS) under specific conditions: initial temperature at 150 °C for 3 min, increasing at 10 °C/min to 190 °C for 5 min, then at 5 °C/min to 220 °C for 16 min. Mass spectra conditions included an MS transfer line temperature of 250 °C, ion source temperature of 220 °C, ionization mode: EI, ion polarity: positive, and scan time: 0.2 s[7]. The purified c9,t11,c15-CLNA were then dissolved in 10% skim milk powder for gavage[7].

2.2 Animal management and experimental procedures

A total of 56 C57BL/6N mice (25 males, 31 females; 6–8 weeks old; 15–19 g body weight) were used for acute and subchronic toxicity testing of c9,t11,c15-CLNA. Mice were housed in accredited SPF facilities (license SYXK(Su)-2021-0056). The barrier environment met conditions including a temperature of 20–26 °C, relative humidity of 40%–70%, noise below 60 dB, and 12-h light-dark cycles with an illuminance intensity in dark places of 10-20LX[7]. The animals were fed normal rodent maintenance feed provided by Jiangsu Co-creation Pharmaceutical Biotechnology Co., Ltd., containing 18.6% crude protein, 4.8% crude fat, and 60% carbohydrates. The experimental design followed OECD guidelines 425 and 407 (Fig. 1A)[10-11]. LD_{50} data were obtained through acute toxicity tests to design subsequent subchronic toxicity tests based

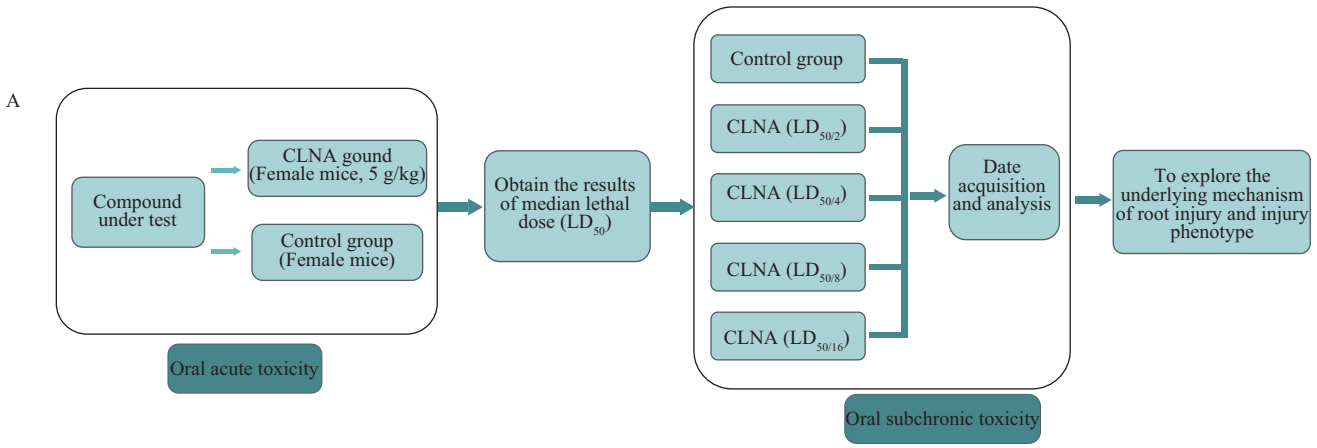

Fig. 1 The figure displays the experimental flow and mass spectrometry information of c9,t11,c15-CLNA. (A) Flowchart of the entire experiment. (B, C) Mass spectrometry data for c9,t11,c15-CLNA; (B) Total ion current diagram. (C) Mass spectrometry fragment information diagram for c9,t11,c15-CLNA, with the horizontal axis ranging from 30 to 300 Da.

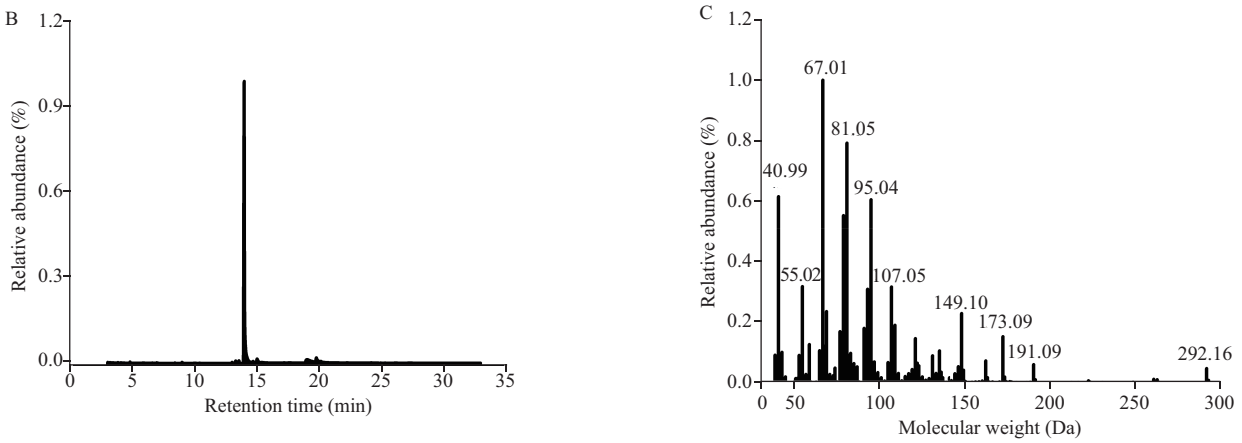

Fig. 1 (*Continued*)

on LD_{50} values. A 12-week experiment was conducted according to corresponding gavage doses to collect parameters such as body weight, organ coefficient, blood indicators, biochemistry, and tissue pathology to determine the toxicity range. The animal ethics number for this study was JN.No20211130c0600429[470].

2.3 Acute toxicity test

Acute toxicity was evaluated with single-dose administration (control group *vs*. group receiving 5 g/kg) followed by monitoring for 14 days post-dose to assess mortality[10]. Before gavage, mice were fasted for 12 h with food provided 2 h after administering the test substance. Observations of gait, fur condition, feces quality, and neurological reflexes were made at intervals ranging from 30 min to 72 h post-gavage (0.5, 1, 2, 4, 8, 12, 24, 48, and 72 h); abnormalities prompted a pole-climbing test. After the 14-day acute toxicity test period, LD_{50} data were obtained along with measurements of mortality rates, body weight changes, and organ coefficients for the heart, liver, brain, spleen, lung, kidney, and ovary.

2.4 Subchronic toxicity test

2.4.1 Changes in body weight and organ coefficients

Based on the previously obtained LD_{50}, we conducted subchronic toxicity testing at doses of $LD_{50/2}$, $LD_{50/4}$, $LD_{50/8}$, and $LD_{50/16}$, referring to the OECD407 standard[11]. The experiment spanned 12 weeks. We weighed the animals biweekly and, on the final day of the experiment, fasted the mice for 12 h before recording their final weight. Subsequently, we collected mouse blood and excised their heart, liver, brain, spleen, lung, kidney, testis, and ovary organs. We later calculated the corresponding organ coefficients.

2.4.2 Hematology testing, plasma biochemistry testing and histopathology analysis

We collected mouse blood via orbital bleeding into anticoagulant tubes containing lithium heparin (10 IU/mL). A fully automatic blood cell analyzer (Shenzhen Mindray Bio-Medical Electronics Co., Ltd., BC-5000 Vet) provided data on immune cell counts, red blood cell and hemoglobin-related indicators, and platelet values. Immune cell count indicators included white blood cell (WBC), neutrophil count (Neu#), lymphocyte count (Lym#), monocyte count (Mon#), neutrophil percentage (Neu%), lymphocyte percentage (Lym%), and monocyte percentage (Mon%). Red blood cell and hemoglobin-related indicators were red blood cell count (RBC), hemoglobin concentration (HGB), hematocrit (HCT), mean corpuscular volume (MCV), mean corpuscular hemoglobin (MCH), mean corpuscular hemoglobin concentration (MCHC), and platelet count (PLT). After blood cell analysis, we prepared plasma by centrifuging blood samples at 3 500 r/min for 15 min at 4 °C and collected the supernatant. A biochemical analyzer (Shenzhen Mindray Bio-Medical Electronics Co., Ltd., BS-480) measured liver function, kidney function, blood glucose and lipid indicators, and inorganic ion concentration. Liver function tests included total protein (TP), albumin (ALB), alanine transaminase (ALT), and aspartate transaminase (AST). Kidney function tests measured urea nitrogen (Urea-N) and creatinine (CRE). Blood glucose and lipid indicators were glucose (Glu), triglyceride (TG), total cholesterol (TC), high-density lipoprotein cholesterol (HDL-C), and low-density lipoprotein cholesterol (LDL-C). Inorganic ion concentration tests measured calcium (Ca), phosphorus (P), potassium (K), sodium (Na), and chloride (Cl). After collecting animal organ coefficients, we fixed tissues in 4% polyformaldehyde for 24 h before sectioning. We dehydrated tissues with ethanol of increasing concentration, replaced ethanol with xylene, and embedded them in paraffin. After cooling, we sectioned the embedded blocks to a thickness of 2 μm. Hematoxylin and eosin staining followed, with sections sealed on glass slides[7]. A digital slide scanner (Hungary 3DHISTECH Co., Ltd. PANNORMIC MIDI) scanned the sections for tissue morphology analysis. Assign corresponding histopathological scores to the abnormalities observed in tissue sections.

2.5 Cell-based experiments

2.5.1 c9,t11,c15-CLNA and PPAR-γ protein molecular docking

We obtained the human PPAR-γ structure (ID:3ADT) from the Research Collaboratory for Structural Bioinformatics (RCSB) and selected chain A for molecular docking studies. Using Avogadro, we acquired the 3D structure of c9,t11,c15-CLNA and optimized it with General AMBER Force Field. Before docking with Auto Dock Tools

(ADT version 1.5.7), we added non-polar hydrogen and Gasteiger charges to the protein and ligand. We defined the center coordinates of the PPAR-γ active pocket as x = 14.8Å, y = 62.3Å, z = 9.5Å, with dimensions of 31.2 × 24.3 × 24.0 Å based on Waku et al.[12]. Vina software performed molecular docking; PyMOL 2.5 (Open-source, Schrödinger, New York, USA) and Discovery Studio Visualizer Client (Open-source, BIOVIA, San Diego, USA) analyzed results.

2.5.2 Cell cultivation

HepG2 liver cells, provided by the Shanghai Institute of Cellular Sciences, Chinese Academy of Sciences, were employed in this study. The cell culture techniques were primarily based on the protocols described by Ren et al.[8]. The cells were maintained in DMEM medium supplemented with 10% fetal bovine serum and 1% antibiotics (streptomycin and penicillin) at 37 °C with a 5% CO_2 atmosphere. Cells were seeded in 10 cm diameter culture dishes (Fisher, Ottawa, ON, Canada), with the medium refreshed every 48 h. Upon reaching 80%–95% confluence, cells were passaged. Prior to passaging, cell morphology and density were assessed under a microscope to ensure suitability for subculturing. For passaging, cells were initially digested with trypsin; Subsequently, remove trypsin and 3 mL of pre-warmed (37 °C) medium was added and blown apart the cells. The resulting cell suspension was transferred to a 15 mL sterile centrifuge tube and centrifuged at 1 000 × g for 5 min. After discarding the supernatant, fresh medium was used to resuspend the cells. Cell concentration and number were then adjusted according to the specific requirements of each experiment.

2.5.3 Excessive c9,t11,c15-CLNA induces lipid accumulation in HepG2 cells

To prepare the c9,t11,c15-CLNA solution, the pH of DMEM medium containing 10% BSA was adjusted to 10 before adding c9,t11,c15-CLNA (final concentration of 1 mmol/L, dissolved in 1 mmol/L sodium hydroxide solution)[8]. The mixture was subjected to ultrasonic treatment in a 37 °C water bath until bubbles formed upon shaking, at which point ultrasonication was halted. The pH was then adjusted to between 7.2 and 7.4 to obtain the c9,t11,c15-CLNA stock solution. The maximum tolerated dose of c9,t11,c15-CLNA for HepG2 cells was established using the CCK-8 assay. At this dose, the compound's effect on lipid accumulation in HepG2 cells was investigated. For determining the maximum tolerated dose, HepG2 cells were counted and seeded into a 96-well plate (utilizing only the central 60 wells) at a density of approximately 10 000 cells per well in 200 μL of DMEM medium. After a 24-h incubation at 37 °C with 5% CO_2 to facilitate cell adhesion, varying concentrations of c9,t11,c15-CLNA were administered, followed by another 24-h culture period. The CCK-8 kit instructions were followed to assess cell viability and establish the maximum tolerated dose[13]. At this dose, lipid accumulation assays were performed on HepG2 cells seeded into a 6-well plate at approximately 200 000 cells per well in 2 mL of DMEM medium. The lipid accumulation experiment consisted of 3 groups: a control group, a treatment group, and a treatment group with the GW9662 inhibitor. Cells were seeded in 6-well plates and allowed to attach for 24 h. The control group was then treated with the vehicle solution, while the treatment group received the specified concentration of c9,t11,c15-CLNA. In the treatment group with the GW9662 inhibitor, cells were allowed to attach for 20 h before being pre-treated with 5 μmol/L of GW9662 for 4 h. After 24 h of culture, cells from all groups were harvested for experimental data analysis.

2.5.4 Measurement of lipid deposition

The objective of this experiment was to quantify c9,t11,c15-CLNA-induced lipid deposition in cells and investigate potential target protein effects using cell staining, Western blot (WB), and other techniques. The procedure for quantifying lipid accumulation was as follows: cells treated with c9,t11,c15-CLNA were washed thrice with PBS and fixed with 4% paraformaldehyde for 10 min. They were then permeabilized with 0.1% Triton X-100 for 15 min at room temperature[14]. Nile red working solution and Hoechst's working solution were added and incubated for 15 min in a cell culture incubator, with agitation every 5 min[14-15]. The working solutions of Nile red and Hoechst were prepared by diluting their respective 1 mmol/L stock solutions with serum-free DMEM at a ratio of 1:1 000. Afterward, cells were washed 3 times with serum-free DMEM medium and examined using a Zeiss laser confocal microscope (LSM880, Carl Zeiss AG, Germany).

Protein detection methods were employed to determine the expression of potential target proteins and to verify with the corresponding inhibitor: SDS-PAGE and Western blot were used to separate and detect proteins in cells. RIPA lysis buffer and protease inhibitor (protease and phosphorylation inhibitor) were utilized to lyse the cells and extract proteins[16]. The cells induced by c9,t11,c15-CLNA were washed 3 times with PBS, and 200 μL of RIPA lysis buffer and protease inhibitor were added to each well. The cells were lysed by ultrasound on ice, with an ultrasonic intensity of 30%, on for 3 s and off for 4 s, for a total of 1 min. Then 5 × Loading buffer was added to 200 μL of lysis buffer, mixed well, and boiled for 10 min at 100 °C. After centrifugation, SDS-PAGE was performed to separate the proteins. The gel was then transferred to a PVDF (infiltrated with methanol) membrane using a membrane transfer device. After blocking with skim milk for 1 h, the corresponding primary antibody was added and incubated overnight at 4 °C in a chromatography cabinet. The membrane was subsequently washed 3 times with TBST, and the corresponding secondary antibody was added and incubated at room temperature for 1 h. Finally, protein expression was detected with a chemiluminescent staining solution. The WB procedure primarily referred Vallejo-Illarramendi et al.[16].

2.6 Data analysis

All data were analyzed and plotted using GraphPad Prism 8.0 Windows software (GraphPad software, San Diego, USA). Data were presented as mean ± SD. A One-way analysis of variance (ANOVA) was used to test the significance. * in tables and figures indicated significant differences between groups and their corresponding gender-matched controls, $P \leq 0.05$.

3. Results and discussion

3.1 Acute toxicity test results of c9,t11,c15-CLNA

This experiment first performed substance identification of the extracted compound, confirming that its parent ion mass-to-charge ratio (*m/z* 292.16) and the type and intensity of secondary mass spectrometry fragments were consistent with those of the previously identified compound, as shown in Figs. 1B and C[17-18]. The prepared c9,t11,c15-CLNA was then used for subsequent experiments. The acute toxicity test aimed to observe acute poisoning reactions and obtain the LD_{50} of animals receiving excessive test substances, providing a reference for subsequent observation indicators and subchronic toxicity test dose selection. The international standard OECD 425 was utilized for acute toxicity testing. The guideline recommends an initial conventional dose of 2 000 mg/kg to commence the experiment. However, the consumption history of analogs of c9,t11,c15-CLNA indicates a relatively broad range of safe doses. Consequently, the maximum recommended dose of 5 000 mg/kg, as specified in the guidelines, was employed for the study. Female mice were selected as experimental animals due to their typically higher sensitivity. The results indicated that a single dose of 5 000 mg/kg c9,t11,c15-CLNA did not cause animal mortality within 15 days (Table 1). According to food toxicity grading, compounds with a dose greater than 5 000 mg/kg are considered almost non-acutely toxic, with an LD_{50} greater than 5 000 mg/kg[10,19]. No abnormalities such as gait, hair condition, or neurological reflexes were observed in test animals post-administration, except for slightly thin feces at 8 h that returned to normal after 24 h. Animal weight and organ coefficient data during the acute toxicity test are shown in Table 1, with no significant differences observed. Therefore, c9,t11,c15-CLNA was considered a non-acutely toxic compound. Based on this, doses for the subsequent subchronic toxicity test were designed as $LD_{50/2}$ (2 500 mg/kg), $LD_{50/4}$ (1 250 mg/kg), $LD_{50/8}$ (625 mg/kg), and $LD_{50/16}$ (312.5 mg/kg)[11].

3.2 Changes in body weight, organ coefficients, food and water intake in subchronic toxicity test

In toxicological studies, changes in body weight and organ coefficients are crucial indicators for evaluating the effects of test substances on biological organisms. Typically, changes in body weight are closely related to nutritional status and physiological functions. Organ-to-body weight ratios are generally stable; however, toxic compounds can affect organs, causing congestion, edema, hyperplasia, hypertrophy, or even tissue cell apoptosis, which will impact organ coefficients or body weight[20-21]. These changes can better reflect the comprehensive toxicity of the test substance on organs and provide important clues regarding the target organs of toxic effects based on pathological histological changes[20-21]. These data are listed in Tables 2 and 3. The table shows no significant differences in body weight or organ coefficients for the heart, lungs, kidneys, brain, testes, and ovaries. Significant differences were observed in some groups' liver and spleen coefficients. The liver coefficient increased in both female and male groups at the 2 500 mg/kg dose group, while the spleen coefficient decreased significantly in both female and male groups at the same dose level (Tables 2 and 3). The liver is the primary organ for lipid processing and was significantly up-regulated in the 2 500 mg/kg group, which may be due to lipid metabolism's influence on liver function[22]. Previous studies have also found that c9,t11,c15-CLNA analogues affect the immune system, potentially leading to spleen damage[3]. However, the organ coefficients only reflect changes in the weight of the organs and do not identify the specific damage that may have occurred in the liver and spleen. Further verification is needed to confirm whether these changes are consistent with pathological alterations.

Table 1
Body weight and organ coefficients of mice in acute toxicity.

Group	Initial weight (g)		Final weight (g)		Brain (mg/g)		Hepatic (mg/g)		Spleen (mg/g)		Heart (mg/g)		Lung (mg/g)		Kidney (mg/g)		Ovary (mg/g)	
	Control	5 g/kg	Control	5 g/kg	Control	5 g/kg	Control	5 g/kg	Control	5 g/kg	Control	5 g/kg	Control	5 g/kg	Control	5 g/kg	Control	5 g/kg
Median	15.14	15.42	17.24	17.39	23.34	24.73	53.09	57.05	3.83	4.26	6.12	6.48	8.15	8.37	16.59	16.68	0.62	0.66
Mean	15.45	15.29	17.70	17.29	23.55	24.31	54.11	56.87	3.87	4.12	6.14	6.42	7.98	8.34	16.59	16.48	0.60	0.64
SD	0.81	0.53	0.88	0.64	0.72	1.23	2.93	1.02	0.25	0.30	0.08	0.37	0.32	0.04	0.25	0.36	0.06	0.07
Minimum	14.84	14.71	17.14	16.61	22.97	22.93	51.82	55.78	3.64	3.77	6.07	6.02	7.61	8.29	16.34	16.07	0.53	0.56
Maximum	16.37	15.76	18.72	17.88	24.36	25.29	57.420	57.80	4.14	4.34	6.24	6.76	8.18	8.38	16.84	16.71	0.65	0.70

Note: Summarizes the acute toxicity study results, including the change of body weight and organ coefficients. Results are expressed as mean ± SD (male/female $n = 3$). *Represents a significant difference compared to the control group, $P < 0.05$.

Table 2
Changes in body weight of mice in subchronic toxicity.

Gender	Group	Initial weight (g)	2 weeks weight (g)	4 weeks weight (g)	6 weeks weight (g)	8 weeks weight (g)	10 weeks weight (g)	12 weeks weight (g)
Female	Control	17.61 ± 0.99	18.63 ± 1.09	19.78 ±1.23	20.44 ± 1.18	22.5 ± 1.14	23.37 ± 1.04	24.32 ± 0.98
	312.5 mg/kg	17.4 ± 0.55	18.49 ± 0.74	19.86 ± 0.84	20.65 ± 1.02	22.45 ± 1.22	23.47 ± 1.05	24.16 ± 1.07
	625 mg/kg	17.10 ± 1.10	18.50 ± 0.69	19.65 ± 1.13	20.83 ± 0.78	22.45 ± 0.9	23.63 ± 0.85	24.13 ± 0.86
	1 250 mg/kg	17.50 ± 0.72	18.51 ± 0.66	20.05 ± 1.29	20.76 ± 0.89	22.14 ± 1.31	23.03 ± 1.43	23.54 ± 1.46
	2 500 mg/kg	17.83 ± 0.76	18.47 ± 0.76	19.87 ± 0.97	20.54 ± 0.94	21.71 ± 0.9	22.45 ± 0.8	22.98 ± 0.94
Male	Control	18.73 ± 1.39	21.09 ± 1.16	23.68 ± 1.15	25.09 ± 1.52	28.39 ± 1.64	30.08 ± 1.45	31.18 ± 1.65
	312.5 mg/kg	19.08 ± 0.92	21.47 ± 1.15	23.48 ± 1.14	25.06 ± 1.62	28.03 ± 1.66	29.83 ± 2.17	31.24 ± 1.78
	625 mg/kg	18.86 ± 1.02	21.23 ± 1.22	23.76 ± 1.52	25.41 ± 1.56	27.92 ± 1.36	29.95 ± 1.45	31.04 ± 1.48
	1 250 mg/kg	18.68 ± 1.39	21.06 ± 0.72	23.56 ± 1.47	25.01 ± 1.16	27.28 ± 1.15	29.15 ± 1.45	30.49 ± 1.1
	2 500 mg/kg	18.45 ± 1.22	21.25 ± 0.96	22.84 ± 0.95	23.96 ± 1.26	26.32 ± 1.51	27.72 ± 1.38	29.41 ± 1.41

Note: Presents the results of the subchronic toxicity study, including the findings of body weight. Results are expressed as mean ± SD (male/female $n = 5$). *Represents a significant difference compared to the control group, $P < 0.05$.

Table 3
Changes in organ coefficients of mice in subchronic toxicity.

Gender	Group	Heart (mg/g)	Hepatic (mg/g)	Brain (mg/g)	Spleen (mg/g)	Lung (mg/g)	Kidney (mg/g)	Ovary (mg/g)	Testis (mg/g)
Female	Control	6.42 ± 0.19	52.86 ± 1.44	12.76 ± 0.75	3.33 ± 0.11	6.64 ± 0.47	12.73 ± 1.38	0.74 ± 0.05	
	312.5 mg/kg	6.50 ± 0.27	50.14 ± 3.32	12.91 ± 0.67	3.12 ± 0.18	6.79 ± 0.8	12.92 ± 1.4	0.72 ± 0.12	
	625 mg/kg	6.53 ± 0.28	51.76 ± 2.55	12.86 ± 0.77	3.28 ± 0.13	6.72 ± 0.62	12.8 ± 0.74	0.68 ± 0.13	
	1 250 mg/kg	6.64 ± 0.53	53.73 ± 1.76	12.95 ± 1.05	3.13 ± 0.27	6.59 ± 0.72	12.52 ± 0.61	0.71 ± 0.09	
	2 500 mg/kg	6.75 ± 0.17	57.65 ± 1.43*	12.92 ± 0.70	3.03 ± 0.19*	7.15 ± 0.87	12.58 ± 0.87	0.74 ± 0.07	
Male	Control	6.41 ± 0.15	53.18 ± 1.66	13.28 ± 0.78	3.66 ± 0.32	5.63 ± 0.36	13.26 ± 1.26		5.59 ± 0.26
	312.5 mg/kg	6.45 ± 0.14	51.97 ± 1.02	12.88 ± 0.83	3.51 ± 0.51	5.36 ± 0.31	13.12 ± 0.89		5.53 ± 0.16
	625 mg/kg	6.63 ± 0.17	51.66 ± 4.18	13.07 ± 0.58	3.31 ± 0.14	5.54 ± 0.31	13.12 ± 0.65		5.89 ± 0.16
	1 250 mg/kg	6.67 ± 0.4	54.71 ± 2.79	13.38 ± 0.71	3.53 ± 0.21	5.59 ± 0.7	12.91 ± 0.44		5.86 ± 0.26
	2 500 mg/kg	6.68 ± 0.57	57.38 ± 2.53*	13.43 ± 0.69	3.25 ± 0.20*	5.8 ± 0.77	13.22 ± 1.06		5.86 ± 0.29

Note: Presents the results of the subchronic toxicity study, including the results of organ coefficients. Results are expressed as mean ± SD (male/female $n = 5$). *Represents a significant difference compared to the control group, $P < 0.05$. Groups were control, 312.5, 625, 1 250 and 2 500 mg/kg.

3.3 Changes in blood and biochemical parameters

In this study, we employ blood tests and biochemical tests, both of which are crucial in toxicological investigations[23-24]. These indicators often change before organ function is significantly impaired, as organ coefficients can only indicate organ enlargement or atrophy[23-24]. Blood cell analysis can reveal variations in the number, morphology, and function of blood cells, potentially indicating impacts on organismal health such as immune system function and nutritional status[24]. This study focused on WBC count, WBC differential count, red blood cells, hemoglobin, and platelets[24-25]. The results, presented in Table 4, revealed significant differences in MCV between the 2 500 mg/kg dose groups for both male and female mice and their respective control groups. Similarly, MCHC showed significant differences at 1 250 and 2 500 mg/kg doses in male mice and at the 2 500 mg/kg dose in female mice compared to their sex-matched control groups. The abnormal indicators were MCV and MCHC, with no significant differences observed in other parameters. MCV indicates the average volume of individual red blood cells, which helps assess red blood cell size and potential anemia[24-25]. MCHC measures the concentration of hemoglobin within red blood cells[24-25]. The observed decrease in MCV and increase in MCHC could potentially be due to malnutrition in mice caused by high concentrations of c9,t11,c15-CLNA. Generally, these changes are thought to be indicative of anemia, which can result from digestive system damage, impaired nutrient reabsorption due to kidney damage, or reduced nutrient synthesis capacity due to liver damage[24-25]. According to current literature, a decrease in RBC or HGB is the reference value for anemia, while MCV and MCHC are the indicators used to classify anemia[24-25]. Thus, the abnormal MCV and MCHC values observed in this study could potentially be false positives caused by excessive lipid intake[26]. Therefore, the mice may not be anemic as a result of the c9,t11,c15-CLNA overdose, but rather the abnormal MCV and MCHC values due to other factors. This cannot be determined solely from the blood data and requires analysis in conjunction with additional data.

Biochemical parameters serve as another critical indicator, reflecting an individual's blood metabolism and internal environment stability, and assessing the impact of toxins on murine health[23]. For instance, liver function markers, kidney function markers, and blood lipid markers provide insights into the functioning and extent of damage to vital organs such as the liver and kidneys[11,26-27]. The results indicated significant differences in TP and ALB levels in the 2 500 mg/kg male group compared to the control group (Table 5). Alanine aminotransferase (ALT) levels were significantly different in the 1 250 and 2 500 mg/kg female groups and the 2 500 mg/kg male group compared to their respective control groups (Table 5). Additionally, aspartate aminotransferase (AST) levels in the 2 500 mg/kg female group differed significantly from the control group (Table 5). TP represents all proteins, including ALB and globulin, reflecting nutritional status, liver synthetic function, and kidney excretion capacity[28-29]. ALB, synthesized by the liver, is essential for maintaining colloid osmotic pressure and pH in blood vessels, transporting metabolites, and regulating physiological effects[28-29].

Table 4
Blood analysis of mice in subchronic toxicity.

Group	Female					Male				
	Control	312.5 mg/kg	625 mg/kg	1 250 mg/kg	2 500 mg/kg	Control	312.5 mg/kg	625 mg/kg	1 250 mg/kg	2 500 mg/kg
WBC (10^9/L)	5.8 ± 0.86	5.33 ± 0.56	5.84 ± 1.26	5.14 ± 0.44	5.67 ± 1.2	6.16 ± 0.72	5.9 ± 0.64	5.67 ± 0.77	6.02 ± 0.91	6.21 ± 1.21
Neu# (10^9/L)	0.85± 0.12	0.82 ± 0.05	0.94 ± 0.26	0.8 ± 0.19	0.86 ± 0.2	1.01 ± 0.21	0.99 ± 0.18	1.01 ± 0.18	1.09 ± 0.39	1.11 ± 0.24
Lym# (10^9/L)	4.63 ± 0.8	4.2 ± 0.56	4.56 ± 1.05	4.04 ± 0.25	4.5 ±0.98	4.7 ± 0.58	4.49 ± 0.72	4.26 ± 0.72	4.53 ± 0.98	4.7 ± 0.92
Mon# (10^9/L)	0.17 ± 0.02	0.17 ± 0.03	0.17 ± 0.06	0.15 ± 0.02	0.17 ± 0.04	0.18 ± 0.05	0.18 ± 0.07	0.17 ± 0.06	0.19 ± 0.07	0.18 ± 0.04
Neu%	14.84 ± 2.24	15.56 ± 2	16.18 ± 3.53	15.34 ± 2.65	15.2 ± 1.99	16.42 ± 2.88	17.06 ± 3.9	18.16 ± 4.01	18.6 ± 6.9	17.86 ± 1.48
Lym%	79.56 ± 2.46	78.7 ± 2.25	77.9 ± 3.42	78.7 ± 2.61	79.38 ± 2.3	76.44 ± 3.93	75.78 ± 4.1	74.86 ± 3.59	74.82 ± 5.96	75.64 ± 2.29
Mon%	3.00 ± 0.29	3.16 ± 0.57	2.84 ± 0.67	2.88 ± 0.49	2.92 ± 0.19	2.96 ± 0.54	3.16 ± 1.35	3.1 ± 1.07	3.16 ± 0.77	3.00 ± 0.66
RBC (10^{12}/L)	8.55 ± 0.61	8.4 ± 0.55	8.46 ± 0.75	8.33 ± 0.24	8.68 ± 0.8	8.9 ± 0.46	8.85 ± 0.3	9.13 ± 0.48	8.92 ± 0.42	9.00 ± 0.58
HGB (g/L)	126.40 ± 8.29	126.80 ± 5.54	127.00 ± 7.81	125.60 ± 4.16	131.00 ± 10.77	128.80 ± 7.16	132.60 ± 4.34	123.60 ± 12.93	125.40 ± 7.27	130.60 ± 9.66
HCT	0.39 ± 0.02	0.36 ± 0.02	0.36 ± 0.05	0.36 ± 0.01	0.34 ± 0.06	0.4 ± 0.02	0.38 ± 0.01	0.36 ± 0.03	0.36 ± 0.01	0.37 ±0.05
MCV (fL)	45.14 ± 2.02	43.04 ± 0.95	43.45 ± 0.79	43.08 ± 0.75	39.4 ± 5.08*	45.08 ± 2.06	43.28 ± 1.07	39.94 ± 4.01	43.4 ± 3.72	40.98 ± 3.92*
MCH (pg)	14.78 ± 0.51	15.12 ± 0.44	15.06 ± 0.59	15.06 ± 0.11	15.12 ± 0.47	14.5 ± 0.83	15 ± 0.31	13.56 ± 1.59	14.08 ± 1.08	14.52 ± 0.41
MCHC (g/L)	328.2 ± 14.82	350.6 ± 4.39	360.8 ± 32.09	350.00 ± 6.96	389.0 ± 55.89*	321.0 ± 5.92	346.4 ± 7.16	339.2 ± 9.28	355.8 ± 16.36*	356.4 ± 30.66*
PLT (10^9/L)	1 028.4 ± 180.4	1 132.8 ± 266.3	1 062.2 ± 168.0	1 030.6 ± 127.4	1 161.2 ± 189.2	1 307.4 ± 101.9	1 225 ± 188.4	1 288 ± 188.5	1 405 ± 311.8	1 378 ± 365.3

Note: Describes the results of a subchronic toxicity investigation, including the findings of blood analysis. Results are expressed as mean ± SD (male/female $n = 5$). *Represents a significant difference compared to the control group, $P < 0.05$. Recording blood test results in subchronic toxicity experiments.

Table 5
Biochemical data of mice in subchronic toxicity.

Group	Female					Male				
	Control	312.5 mg/kg	625 mg/kg	1 250 mg/kg	2 500 mg/kg	Control	312.5 mg/kg	625 mg/kg	1 250 mg/kg	2 500 mg/kg
TP (g/L)	49.94 ± 5.23	50.08 ± 2.95	50.64 ± 4.93	46.3 ± 4.32	43.8 ± 3.64	51.14 ± 4.02	49.46 ± 2.5	51.38 ± 4.37	48.34 ± 3.97	46.16 ± 3.26*
ALB (g/L)	32.95 ± 5.11	31.54 ± 4.58	32.47 ± 3.46	29.91 ± 3.96	26.78 ± 2.7	31.34 ± 3.02	30.8 ± 2.37	30.85 ± 4.19	31.03 ± 2.76	27.16 ± 2.39*
TG (mmol/L)	1.36 ± 0.14	1.28 ± 0.13	1.31 ± 0.17	1.42 ± 0.14	1.63 ± 0.24	1.6 ± 0.25	1.65 ± 0.26	1.59 ± 0.15	1.69 ± 0.26	1.92 ± 0.21
TC (mmol/L)	3.18 ± 0.63	2.99 ± 0.46	2.86 ± 0.35	3.07 ± 0.56	3.16 ± 0.37	2.95 ± 0.39	2.86 ± 0.42	2.84 ± 0.49	2.85 ± 0.41	3.35 ± 0.48
ALT (U/L)	38.3 ± 6.05	37.1 ± 3.71	40.1 ± 3.95	51.4 ± 8.91*	71.1 ± 6.83*	35.4 ± 8.53	34.9 ± 6.17	40.1 ± 5.91	42.7 ± 5.36	62.6 ± 11.25*
AST (U/L)	112.9 ± 11.71	123.9 ± 6.31	121.1 ± 12.83	132.74 ± 11.82	147.1 ± 18.88*	119.6 ± 8.63	122.5 ± 15.35	112.8 ± 11.75	125.3 ± 18.02	137.5 ± 13.63
HDL-C (mmol/L)	1.25 ± 0.26	1.27 ± 0.16	1.27 ± 0.26	1.26 ± 0.22	1.14 ± 0.15	1.78 ± 0.17	1.64 ± 0.21	1.72 ± 0.48	1.79 ± 0.33	1.46 ± 0.33
LDL-C (mmol/L)	0.39 ± 0.06	0.34 ± 0.07	0.39 ± 0.09	0.4 ± 0.08	0.47 ± 0.1	0.53 ± 0.07	0.51 ± 0.07	0.52 ± 0.1	0.56 ±0.09	0.64 ± 0.09
Glu (mmol/L)	6.95 ± 0.82	6.87 ± 1.39	7.23 ± 0.59	6.78 ± 0.76	7.23 ± 0.61	7.47 ± 0.71	7.35 ± 0.69	7.6 ± 0.8	7.48 ± 0.67	7.64 ± 0.56
Ca (mg/dL)	11.74 ± 0.59	11.44 ± 0.52	11.94 ± 0.9	12.08 ± 1.15	11.98 ± 0.69	11.72 ± 0.77	11.84 ± 1.15	12.14 ± 0.75	12.4 ± 0.97	12.18 ± 1.23
P (mg/dL)	12.26 ± 1.18	12.26 ± 1.32	11.32 ± 1.51	13.28 ± 0.69	11.68 ± 1.26	15.84 ± 1.4	14.18 ±2.22	16.6 ± 1.48	16.18 ± 2.29	15.02 ± 2.61
K (mg/dL)	2.48 ± 0.39	2.6 ± 0.38	2.56 ± 0.38	2.38 ± 0.33	2.3 ± 0.39	2.7 ± 0.2	2.54 ± 0.27	2.68 ± 0.16	2.52 ± 0.47	2.58 ± 0.28
Na (mg/dL)	72.92 ± 4.95	70.92 ± 5.04	71.12 ± 6.84	70.56 ± 5.57	71.26 ± 7.1	70.42 ± 5.33	69.58 ± 2.05	72.56 ± 4.44	70.7 ± 5.33	69.98 ± 3.94
Cl (mg/dL)	43.98 ± 1.8	43.96 ± 2.58	46.12 ± 1.94	45.46 ± 2.28	44.98 ± 3.23	42.5 ± 2.27	43.14 ± 2.23	43.94 ± 2.45	42.9 ± 2.98	44.94 ± 3.06
Urea (mg/dL)	13.44 ± 3.62	11.06 ± 1.52	10.7 ± 2.13	14.44 ± 4.42	13.54 ± 3.88	12.94 ± 2.94	15.64 ± 2.58	13.28 ± 2.83	11.76 ± 1.98	15.92 ± 2.99
CRE (μmol/L)	25.11 ± 5.32	26.77 ± 4.35	27.42 ± 4.86	25.53 ± 1.32	28.15 ± 2.46	27.44 ± 3.33	25.03 ± 4.82	27.51 ± 3.81	27.58 ± 4.21	27.09 ± 3.57

Note: Presents the results of the subchronic toxicity study, including the result of biochemical data. Results are expressed as mean ± SD (male/female $n = 5$). *Represents a significant difference compared to the control group, $P < 0.05$.

Low TP and ALB levels may result from decreased synthesis due to liver cell damage or excessive protein loss after kidney damage[30-31]. However, the main indicators of kidney damage, including CRE, urea and ion levels, did not exhibit substantial changes[30]. Therefore, the decrease in TP and ALB may be attributable to a reduced ability to synthesize proteins following liver injury, and elevated ALT and AST levels may also indicate hepatocyte damage. Additionally, the increase in MCHC could be attributed to heightened lipid levels in the bloodstream[32]. MCHC is calculated based on the relationship between HGB and HCT. It is noteworthy that lipids in the blood can cause an elevated HGB test result, which in turn can lead to an increase in MCHC[32]. While there was no significant difference in TG, it was apparent that TG values increased with higher c9,t11,c15-CLNA concentrations. Meanwhile, there were no significant threats to other blood and biochemical parameters.

3.4 Histopathological evaluation

Histopathological evaluation provided direct observation of tissue cell morphology changes due to c9,t11,c15-CLNA exposure[33-34]. Histopathology is considered the "gold standard" for assessing tissue damage caused by exposure to compounds[33-35]. For instance, liver cell degeneration, lipid accumulation, or glomerular atrophy can be directly observed[33,35]. In this study, sections of the heart, liver, brain, spleen, lungs, kidneys, testes, and ovaries were examined (Fig. 2). The results showed intact structures of the digestive tract and kidneys with no signs of absorption disorder or kidney function impairment (Fig. 2B). However, liver sections exhibited abnormalities in the 2 500 and 1 250 mg/kg groups (Fig. 2A). Circular vacuoles were evident in the hepatocyte cytoplasm, indicating lipid accumulation, and perisinusoidal space outlines were observed in the 1 250 mg/kg group, signaling liver tissue damage (Fig. 2A). We

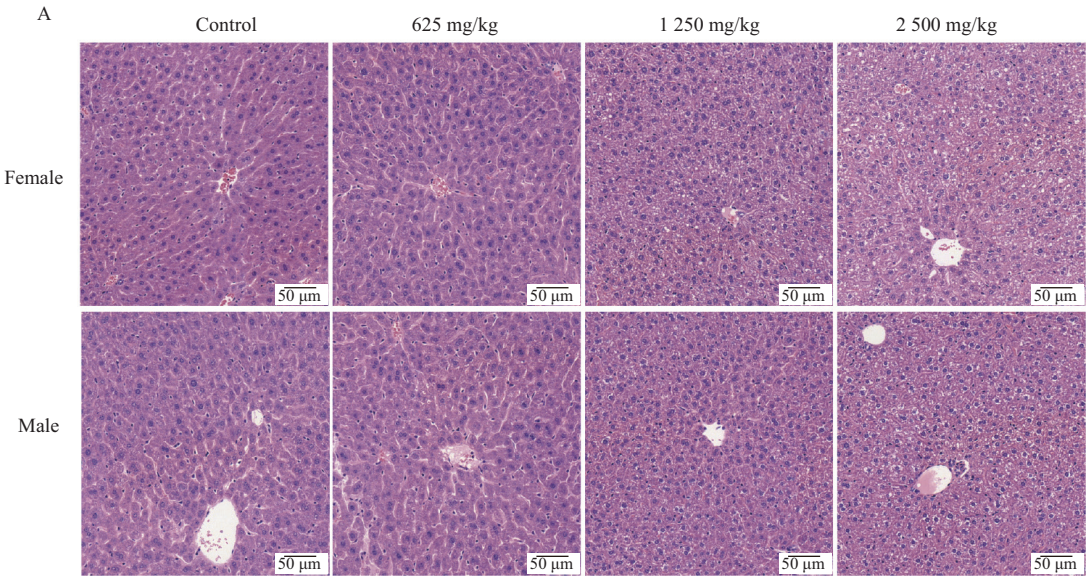

Fig. 2 The figure presents results from molecular docking of c9,t11,c15-CLNA with PPAR-γ. (A) Binding site on PPAR-γ ; (B) 3D binding result between c9,t11,c15-CLNA and PPAR-γ; (C) 2D interaction diagram between c9,t11,c15-CLNA and amino acid residues surrounding PPAR-γ within a 5 Å radius.

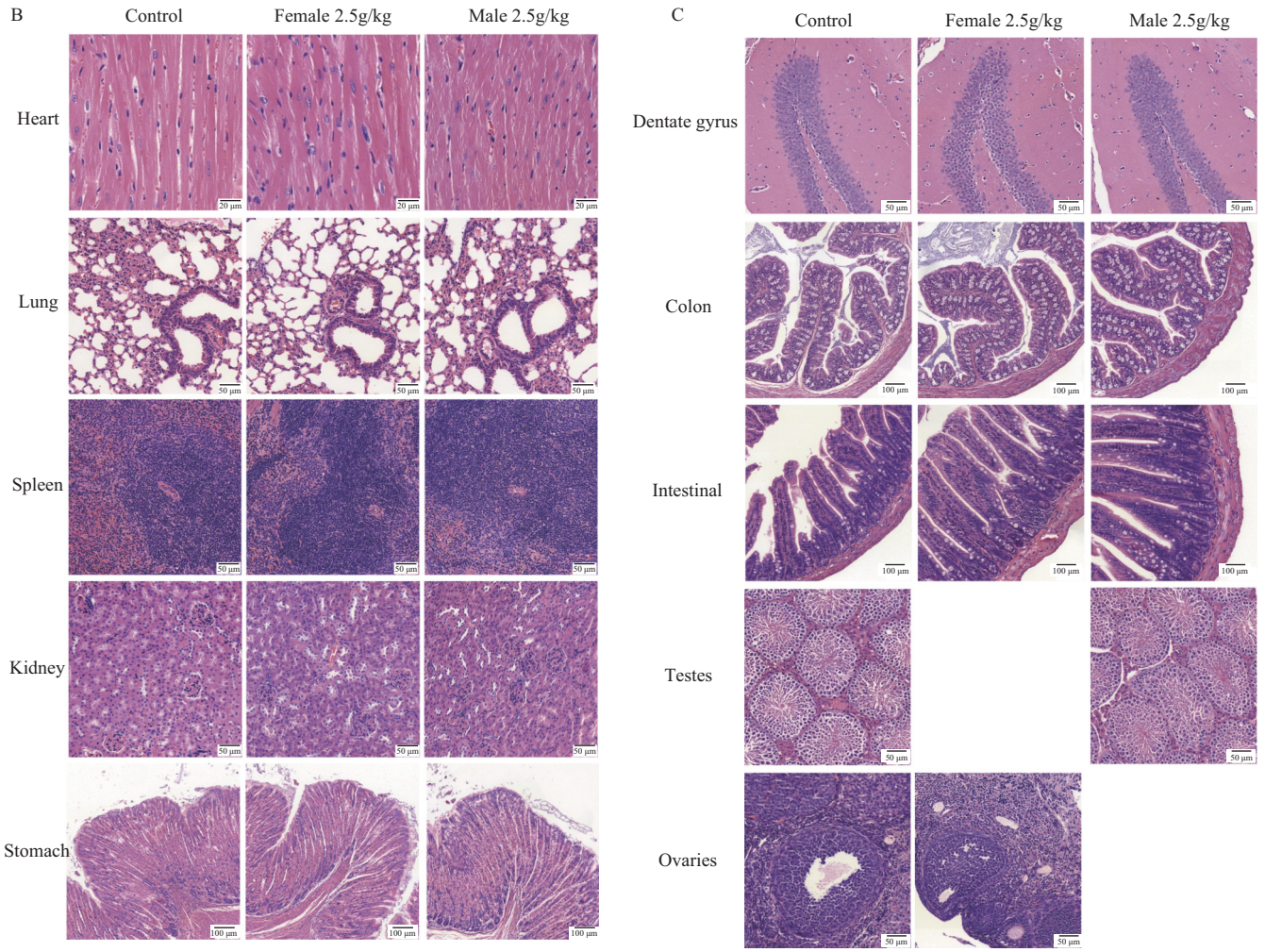

Fig. 2 (*Continued*)

systematically assessed the histopathological slides of the liver using the Steatosis, Activity, Fibrosis (SAF) scoring system proposed by the European Association for the Study of the Liver in 2015[36]. In the SAF scoring system, hepatocellular steatosis is scored 0–3, hepatocellular ballooning degeneration scored 0–2, inflammatory activity scored 0–2, and fibrosis scored 0–4. The histological slides primarily exhibited steatosis and ballooning degeneration. The scoring range for steatosis is 0–3: 0 indicates no steatosis; 1 indicates mild steatosis (1%–33% of hepatocytes); 2 indicates moderate steatosis (34%–66% of hepatocytes); and 3 indicates severe steatosis (67% or more of hepatocytes)[36]. The scoring range for hepatocellular ballooning degeneration is 0–2: 0 indicates no ballooning; 1 denotes mild ballooning (a small number of ballooned hepatocytes); and 2 indicates severe activity (a significant number of ballooned hepatocytes)[36]. After performing SAF analysis on all liver slices, we found that the blank group and the 625 mg/kg group scored 0. In contrast, the 1 250 and 2 500 mg/kg groups received cumulative scores of 1 and 2, respectively, with results being consistent across both sexes. For the other tissues examined, we did not observe any obvious structural changes, cell apoptosis, nuclear condensation, or alterations in intercellular spaces (Figs. 2B and C). Therefore, we did not perform additional quantitative analyses on these tissues. The aforementioned data suggested that increased organ coefficients might be related to liver damage causing lipid accumulation, thus increasing liver weight[22,35]. Biochemical test data supports the notion that liver damage can lead to decreased protein levels by affecting protein synthesis[31]. Additionally, the relative increase in LDL-C and lipid accumulation are also related. Excessive lipid intake may cause excessive lipid accumulation in the liver[37]. The liver may synthesize a large amount of LDL-C to alleviate the pressure caused by lipid accumulation and efficiently transport sufficient lipids to the tissues of the whole body[37]. Although LDL-C did not show significant differences in biochemical results, it exhibited an upward trend. No spleen damage was observed in histological sections; other indicators did not suggest spleen damage either (Fig. 2B). Previous studies have shown that excess lipids can cause splenomegaly[38]. Furthermore, other studies have found that excess lipids can lead to immune abnormalities[39]. These findings suggest that the spleen may be at risk. Although no damage was found in the sections, we classified the 2 500 mg/kg group as potentially detrimental to health due to the abnormalities in the organ coefficients.

In summary, liver damage was observed in the 1 250 and 2 500 mg/kg groups, along with abnormalities in blood indicators, biochemical indicators, and organ coefficients. Consequently, a dose of 625 mg/kg is relatively safe for mice. Utilizing the FDA's guidance document on the maximum recommended starting dose (MRSD) and converting the no observed adverse effect level (NOAEL) from mice to the human equivalent dose (HED) based on body surface area differences

between species, we infer that c9,t11,c15-CLNA is relatively safe for humans at a dose level of 50.62 mg/kg[40]. This provides some reference values for later incorporation and utilization of CLNA in food products. However, it is important to note that these values are only converted and do not indicate the precise amount of c9,t11,c15-CLNA that should be added in human daily diet.

3.5 *Investigation of cellular level mechanisms*

The above study showed some abnormalities in the liver and spleen of mice at a dose of 2 500 mg/kg. The subsequent phase of the study was devoted to the investigation of the underlying mechanisms responsible for liver damage resulting from excessive consumption of c9,t11,c15-CLNA, with the objective of identifying potential mitigation strategies. The decision to exclude the spleen from further investigation was based on the absence of significant morphological abnormalities in histopathological examinations, despite minor alterations in the organ coefficient. In contrast, hepatic tissue demonstrated marked cellular deformation and subtle lipid accumulation. These hepatic alterations prompted our focus on liver pathology, particularly the observed lipid accumulation phenomena. For our experimental model, we selected HepG2 cells. Although derived from hepatocellular carcinoma, HepG2 cells exhibit lipid metabolic pathways analogous to those of normal human hepatocytes, coupled with stable genetic background[41]. These characteristics render HepG2 cells a suitable model for our preliminary investigations.

The PPAR family of proteins plays a crucial role in lipid metabolism regulation. Notable members of this family include PPAR-α, PPAR-γ, and PPAR-β, each with distinct but overlapping functions in lipid homeostasis[3,17]. Among them PPAR-γ overexpression is closely associated with lipid synthesis[17,42]. The PPAR-γ protein exhibits inconsistent effects across various tissues. In adipose tissue, PPAR plays a crucial role in lipid synthesis and enhances insulin sensitivity[42]. However, its overexpression in hepatic tissues promotes the accumulation of intracellular lipids within hepatocytes, resulting in the development of nonalcoholic fatty liver disease (NAFLD), which may subsequently progress to steatohepatitis[43]. Meanwhile, several studies have demonstrated that 18-carbon unsaturated fatty acids, such as *cis*9,*trans*11,*cis*13-CLNA and *cis*9,*trans*11,*trans*13-CLNA, can activate PPAR-γ expression[3]. Therefore, we hypothesize that excessive c9,t11,c15-CLNA may over-activate PPAR-γ, leading to aberrant lipid accumulation in the liver. To test this hypothesis, we employed molecular docking software to determine whether CLNA can bind to the PPAR-γ protein. The PPAR-γ protein activation sites in docking are the binding sites of CYS285, MET364, TYR473, SER289, HIS323, TYR327, LYS367, and HIS449, among others[12,44]. Subsequent cellular experiments confirmed that CLNA can bind to amino acid residues, such as CYS285, MET364, and TYR473, in the PPAR-γ activation site, as shown in Fig. 3[12]. However molecular docking alone cannot accurately reflect the true situation. Therefore, it was essential to verify at the cellular level whether c9,t11,c15-CLNA activate PPAR-γ and lead to lipid accumulation. HepG2 cells, which serve as an experimental model for the liver, were used to determine the maximum safe dose of c9,t11,c15-CLNA for liver cells. This is because the liver is the primary organ affected by excessive intake of this compound. The maximum safe dose of c9,t11,c15-CLNA to cells was obtained from the results of CCK-8 experiments as 80 μmol/L

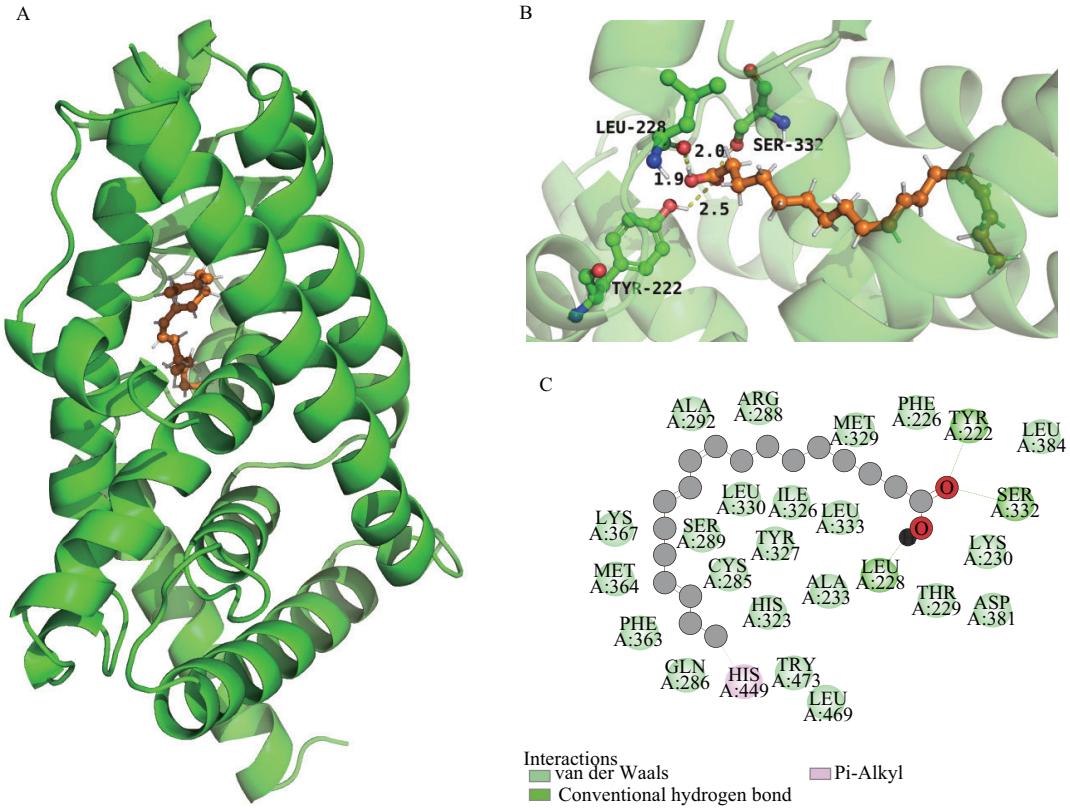

Fig. 3 Molecular docking of c9,t11,c15-CLNA with PPAR-γ. (A) Binding site on PPAR-γ ; (B) 3D binding result between c9,t11,c15-CLNA and PPAR-γ ; (C) 2D interaction diagram between c9,t11,c15-CLNA and amino acid residues surrounding PPAR-γ within a 5 Å radius.

(Fig. 4C). After 24 h of treatment with 80 μmol/L c9,t11,c15-CLNA, HepG2 cells exhibited significant lipid accumulation, positive Nile red staining, and observable lipid droplets under bright-field microscopy. The group treated with the PPAR-γ inhibitor (GW 9662) showed reduced lipid accumulation in Fig. 4A[45]. Furthermore, protein expression analysis indicated that c9,t11,c15-CLNA significantly activated PPAR-γ expression, while the inhibitor group effectively suppressed both PPAR-γ expression and lipid accumulation, as shown in Fig. 4.

In conclusion, our findings suggest that excessive consumption of c9,t11,c15-CLNA can activate PPAR-γ, leading to aberrant lipid accumulation and subsequent liver damage. Therefore, it is crucial to limit the intake of c9,t11,c15-CLNA in daily dietary practices. In the event of an inadvertent overdose of c9,t11,c15-CLNA, PPAR-γ inhibitors could serve as potential antidotes. Concurrently, c9,t11,c15-CLNA can effectively activate PPAR-γ and may be suitable for scenarios that require moderate PPAR-γ activation, such as the treatment of liver fibrosis or diabetes.

4. Conclusion

c9,t11,c15-CLNA is a metabolite of CCFM683, with a safe oral dose for mice determined to be 625 mg/kg, corresponding to a human equivalent dose of 50.62 mg/kg. Doses exceeding 1 250 mg/kg exacerbate liver metabolic disorders in mice. Molecular docking and cellular experiments suggest that liver damage may result from excessive activation of the PPAR-γ protein by overconsumption of c9,t11,c15-CLNA, leading to aberrant lipid accumulation in the liver. The addition of a PPAR-γ inhibitor effectively alleviated lipid accumulation in the liver. These results provide a reference for the safe dosage range and the primary organ-specific toxicity of c9,t11,c15-CLNA consumption, laying a foundation for subsequent applications. Nevertheless, this study has limitations; for instance, it utilized healthy mice, leaving the safety of c9,t11,c15-CLNA for individuals with lipid metabolism disorders, glucose metabolism disorders, or cardiovascular diseases undetermined. These issues warrant further exploration in follow-up research. Moreover, the

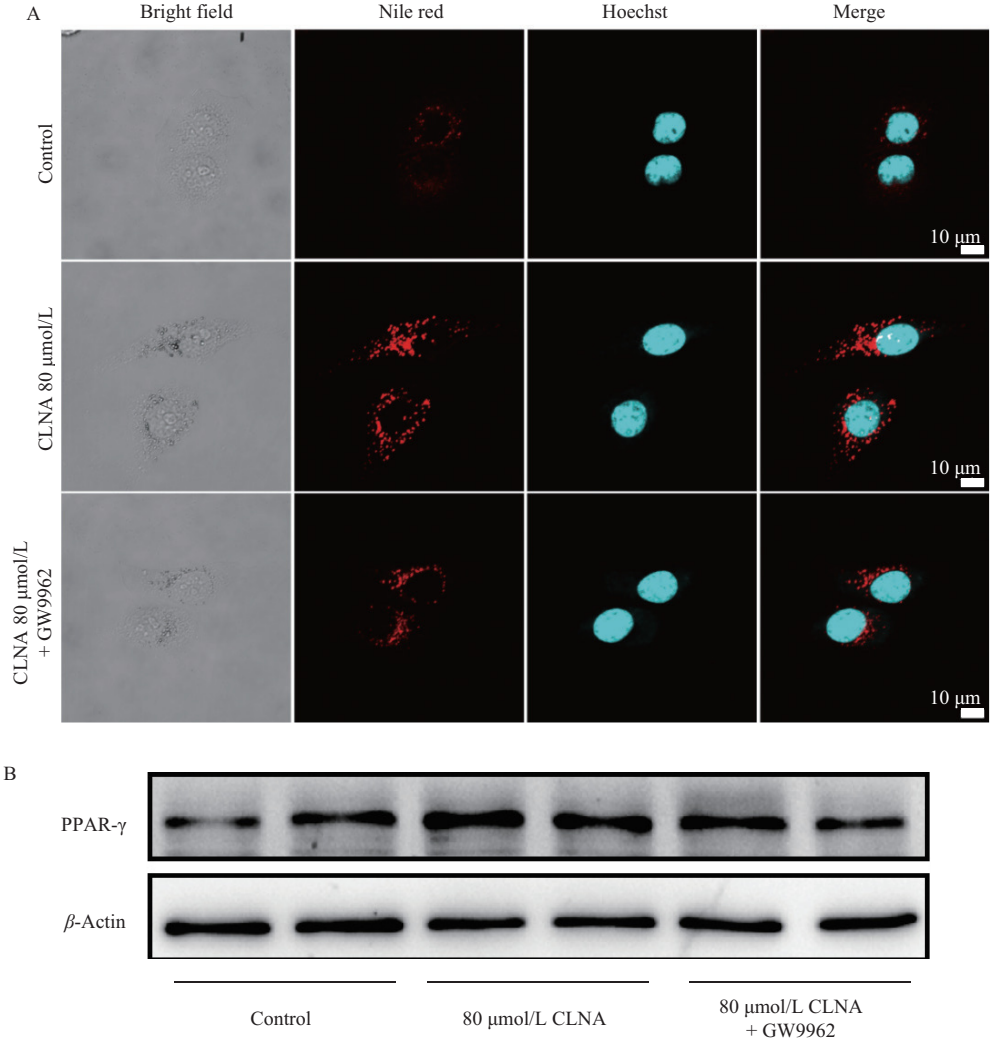

Fig. 4 Lipid accumulation and its potential target protein WB after excessive intake of c9,t11,c15-CLNA. (A) c9,t11,c15-CLNA after excessive intake and stained with Nile red. Bright field means the cell image taken under white light, Nile red group means the lipid image after staining with dye, the brighter the red, the more lipid accumulation. Hoescht group is the stained cell nucleus, which plays the role of locating the cell, merge group is the image of the two groups merged together. (B) Western blot results for PPAR-γ protein expression in cell lysates; *β*-Actin serves as an internal reference protein. Darker bands indicate higher protein expression levels. CLNA represents c9,t11,c15-CLNA, while GW9662 is a specific PPAR-γ inhibitor. (C) Relative content of fluorescence intensity in Fig. C_1, the relative grayscale value in the WB results in Fig. C_2 and toxicity of c9,t11,c15-CLNA on HepG2 cells (CCK-8 method in C_3).

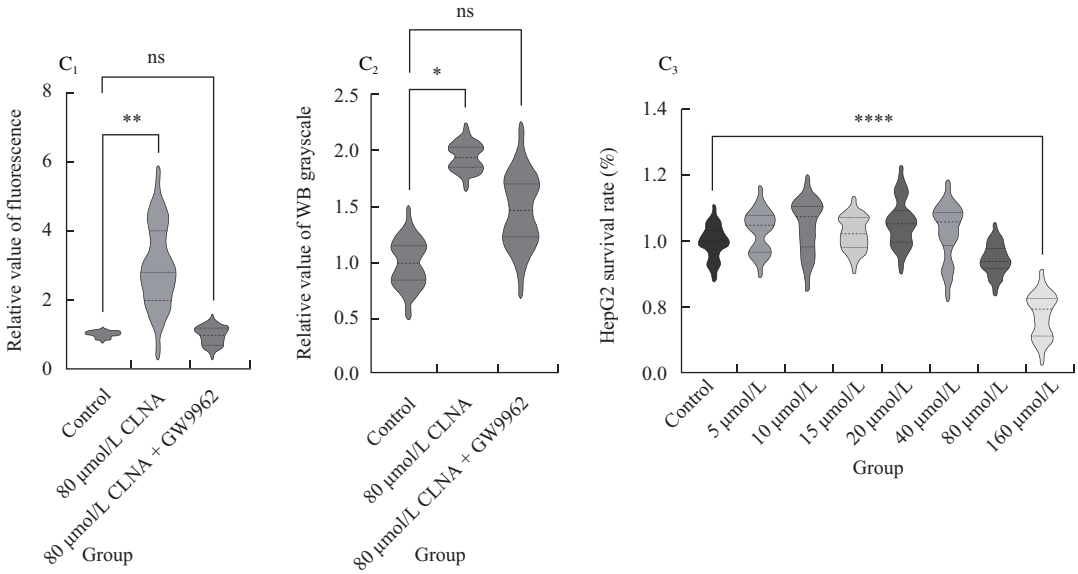

Fig. 4 (*Continued*)

efficacy of PPAR-γ inhibitors was only verified at the cellular level; their ability to alleviate liver damage caused by overconsumption of c9,t11,c15-CLNA *in vivo* remains unclear.

Declaration of interest

The authors declare no conflict of interests.

Acknowledgement

This research was supported by the National Natural Science Foundation of China (32021005, 32072186), the Jiangsu Province "Collaborative Innovation Center for Food Safety and Quality Control" and "the Fundamental Research Funds for the Central Universities".

References

[1] P.C. Calder, Functional roles of fatty acids and their effects on human health, J. Parenter. Enteral. Nutr. 39 (2015) 18S-32S. https://doi.org/10.1177/0148607115595980.

[2] W.S. Harris, T.D. Dayspring, T. Moran, Omega-3 fatty acids and cardiovascular disease: new developments and applications, Postgrad. Med. 125 (2013) 100-113. https://doi.org/10.3810/pgm.2013.11.2717.

[3] M. Du, J. Jin, G. Wu, et al., Metabolic, structure-activity characteristics of conjugated linolenic acids and their mediated health benefits, Crit. Rev. Food Sci. Nutr. (2023) 1-15. https://doi.org/10.1080/10408398.2023.2198006.

[4] G.F. Yuan, X.E. Chen, D. Li, Conjugated linolenic acids and their bioactivities: a review, Food Funct. 5 (2014) 1360-1368. https://doi.org/10.1039/C4FO00037D.

[5] B. Yang, H. Chen, H. Gao, et al., *Bifidobacterium breve* CCFM683 could ameliorate DSS-induced colitis in mice primarily *via* conjugated linoleic acid production and gut microbiota modulation, J. Funct. Foods 49 (2018) 61-72. https://doi.org/10.1016/j.jff.2018.08.014.

[6] H. Gao, B. Yang, C. Stanton, et al., Characteristics of bifidobacterial conjugated fatty acid and hydroxy fatty acid production and its potential application in fermented milk, LWT-Food Sci. Technol. 120 (2020) 108940. https://doi.org/10.1016/j.lwt.2019.108940.

[7] Q. Ren, B. Yang, H. Zhang, et al., c9,t11,c15-CLNA and t9, t11, c15-CLNA from *Lactobacillus plantarum* ZS2058 ameliorate dextran sodium sulfate-induced colitis in mice, J. Agric. Food Chem. 68 (2020) 3758-3769. https://doi.org/10.1021/acs.jafc.0c00573.

[8] Q. Ren, B. Yang, G. Zhu, et al., Antiproliferation activity and mechanism of c9,t11,c15-CLNA and t9, t11, c15-CLNA from *Lactobacillus plantarum* ZS2058 on colon cancer cells, Molecules 25 (2020) 1225. https://doi.org/10.3390/molecules25051225.

[9] K. Parvathi, C. Kandeepan, M. Sabitha, et al., *In-silico* absorption, distribution, metabolism, elimination and toxicity profile of 9,12,15-octadecatrienoic acid (ODA) from *Moringa oleifera*, J. Drug Deliv. Sci. Tec. 12 (2022) 142-150. https://doi.org/10.22270/jddt.v12i2-S.5289.

[10] O.F.E. Co-Operation, Development. Test No. 425: acute oral toxicity: up-and-down procedure, (2008). https://doi.org/10.1787/9789264071049-en.

[11] O.F.E. Co-Operation, Effects. Repeated dose 28-day oral toxicity study in rodents. (2008). https://doi.org/10.1787/9789264304741-en.

[12] T. Waku, T. Shiraki, T. Oyama et al., The nuclear receptor PPAR γ individually responds to serotonin-and fatty acid-metabolites, EMBO J. 29 (2010) 3395-3407. https://doi.org/10.1038/emboj.2010.197.

[13] L. Cai, X. Qin, Z. Xu, et al., Comparison of cytotoxicity evaluation of anticancer drugs between real-time cell analysis and CCK-8 method, ACS Omega 4 (2019) 12036-12042. https://doi.org/10.1021/acsomega.9b01142.

[14] M. Suzuki, Y. Shinohara, T. Fujimoto, Histochemical detection of lipid droplets in cultured cells, Methods Mol. Biol. 931 (2013) 483-491. https://doi.org/10.1007/978-1-62703-056-4_25.

[15] L.C. Crowley, B.J. Marfell, N.J. Waterhouse, Analyzing cell death by nuclear staining with Hoechst 33342, Cold Spring Harb. Protoc. (2016) pdb. https://doi.org/10.1101/pdb.prot087205.

[16] A. Vallejo-Illarramendi, D.K. Marciano, L.F. Reichardt, A novel method that improves sensitivity of protein detection in PAGE and Western blot, Electrophoresis 34 (2013) 1148-1150. https://doi.org/10.1002/elps.201200534.

[17] S. Almoughrabie, L. Cau, K. Cavagnero, et al., Commensal cutibacterium acnes induce epidermal lipid synthesis important for skin barrier function, Sci. Adv. 9 (2023) eadg6262. https://doi.org/10.1126/sciadv.adg6262.

[18] B. Yang, H. Chen, C. Stanton, et al., Mining bifidobacteria from the neonatal gastrointestinal tract for conjugated linolenic acid production, Bioengineered 8 (2017) 232-238. https://doi.org/10.1080/21655979.2016.1222996.

[19] G.L. Kennedy Jr, R.L. Ferenz, B.A. Burgess, Estimation of acute oral toxicity in rates by determination of the approximate lethal dose rather than the LD_{50}, J. Appl. Toxicol. 6 (1986) 145-148. https://doi.org/10.1002/jat.2550060302.

[20] S.E. Lazic, E. Semenova, D.P. Williams, Determining organ weight toxicity with Bayesian causal models: improving on the analysis of relative organ weights, Sci. Rep. 10 (2020) 6625. https://doi.org/10.1038/s41598-020-63465-y.

[21] B. Michael, B. Yano, R.S. Sellers, et al., Evaluation of organ weights for rodent and non-rodent toxicity studies: a review of regulatory guidelines and a survey of current practices, Toxicol. Pathol. 35 (2007) 742-750. https://doi.org/10.1080/019262307015952.

[22] P. Nguyen, V. Leray, M. Diez, et al., Liver lipid metabolism, J. Anim. Physiol. Anim. Nutr. 92 (2008) 272-283. https://doi.org/10.1111/j.1439-0396.2007.00752.x.

[23] S.K. Ramaiah, A toxicologist guide to the diagnostic interpretation of hepatic biochemical parameters, Food Chem. Toxicol. 45 (2007) 1551-1557. https://doi.org/10.1016/j.fct.2007.06.007.

[24] E. Behling-Kelly, Identifying erythrocyte injury in toxicology studies, Toxicol. Pathol. 50 (2022) 883-885. https://doi.org/10.1177/019262332211279.

[25] M. Zandecki, F. Genevieve, J. Gerard, et al., Spurious counts and spurious results on haematology analysers: a review. Part II: white blood cells, red blood cells, haemoglobin, red cell indices and reticulocytes, Int. J. Lab. Hematol. 29 (2007) 21-41. https://doi.org/10.1111/j.1365-2257.2006.00871.x.

[26] S. Pabón-Rivera, R.R. Flores, M. Frei-Jones, The complete blood count: a practical tool for the pediatrician, Pediatr. Rev. 44 (2023) 363-382. https://doi.org/10.1542/pir.2021-005273.

[27] E. Sümer, G.E. Senturk, Ö.U. Demirel, et al., Comparative biochemical and histopathological evaluations proved that receptacle is the most effective part of *Cynara scolymus* against liver and kidney damages, J. Ethnopharmacol. 249 (2020) 112458. https://doi.org/10.1016/j.jep.2019.112458.

[28] T. Hollmén, J.C. Franson, M. Hario, et al., Use of serum biochemistry to evaluate nutritional status and health of incubating common eiders (*Somateria mollissima*) in Finland, Physiol. Biochem. Zool. 74 (2001) 333-342. https://doi.org/10.1086/320421.

[29] D.G. Levitt, M. Levitt, Human serum albumin homeostasis: a new look at the roles of synthesis, catabolism, renal and gastrointestinal excretion, and the clinical value of serum albumin measurements, Int. J. Gen. Med. (2016) 229-255. https://doi.org/10.2147/IJGM.S102819.

[30] E. Kwiatkowska, L. Domański, V. Dziedziejko, et al., The mechanism of drug nephrotoxicity and the methods for preventing kidney damage, Int. J. Mol. Sci. 22 (2021) 6109. https://doi.org/10.3390/ijms22116109.

[31] X.W. Li, R. Zhu, B. Li, et al., Mechanism underlying carbon tetrachloride-inhibited protein synthesis in liver, World J. Gastroenterol. 16 (2010) 3950-3956. https://doi.org/10.3748/wjg.v16.i31.3950.

[32] N.A. Martina, Haematological parameters and their correlation with lipid profile in type 2 diabetes mellitus patients, IOSR J. Nurs. Health Sci. 17 (2018) 283. https://doi.org/10.9790/1959- 1101050106.

[33] C.R. Silva-Correa, V.E. Villarreal-La Torre, A.D. González-Siccha, et al., Acute toxicity of aqueous extract of *Ambrosia arborescens* Mill. on biochemical and histopathological parameters in rats, Toxicol. Res. 38 (2022) 225-233. https://doi.org/10.1007/s43188-021-00106-0.

[34] W. Yao, J. Cheng, A.D. Kandhare, et al., Toxicological evaluation of a flavonoid, chrysin: morphological, behavioral, biochemical and histopathological assessments in rats, Drug Chem. Toxicol. 44 (2021) 601-612. https://doi.org/10.1080/01480545.2019.1687510.

[35] M. Naguib, U.M. Mahmoud, I.A. Mekkawy, et al., Hepatotoxic effects of silver nanoparticles on *Clarias gariepinus*; Biochemical, histopathological, and histochemical studies, Toxicol. Rep. 7 (2020) 133-141. https://doi.org/10.1016/j.toxrep.2020.01.002.

[36] H.H.W. Leung, P. Puspanathan, A.W.H. Chan, et al., Reliability of the nonalcoholic steatohepatitis clinical research network and steatosis activity fibrosis histological scoring systems, J. Gastroenterol. Hepatol. 37 (2022) 1131-1138. https://doi.org/10.1111/jgh.15843.

[37] X. Jin, S. Yang, J. Lu, et al., Small, dense low-density lipoprotein-cholesterol and atherosclerosis: relationship and therapeutic strategies, Front. Cardiovasc. Med. 8 (2022) 804214. https://doi.org/10.3389/fcvm.2021.804214.

[38] B.Z. Altunkaynak, E. Ozbek, M.E. Altunkaynak, A stereological and histological analysis of spleen on obese female rats, fed with high fat diet, Saudi. Med. J. 28 (2007) 353.

[39] S.K. Boi, C.M. Buchta, N.A. Pearson, et al., Obesity alters immune and metabolic profiles: new insight from obese-resistant mice on high - fat diet, Obesity 24 (2016) 2140-2149. https://doi.org/10.1002/oby.21620.

[40] D.B. Colagiovanni, M.A. Peraza, The preparation of a preclinical dossier to support an investigational new drug application and first-in-human clinical trial, A Comprehensive Guide to Toxicology in Nonclinical Drug Development (2024) 199-226. https://doi.org/10.1016/B978-0-323-85704-8.00020-7.

[41] J.R. Wiśniewski, A. Vildhede, A. Norén, et al., In-depth quantitative analysis and comparison of the human hepatocyte and hepatoma cell line HepG2 proteomes, J. Proteomics 136 (2016) 234-247. https://doi.org/10.1016/j.jprot.2016.01.016.

[42] L. Orliaguet, E. Dalmas, K. Drareni, et al., Mechanisms of macrophage polarization in insulin signaling and sensitivity, Front. Endocrinol. 11 (2020) 62. https://doi.org/10.3389/fendo.2020.00062.

[43] H. Chen, H. Tan, J. Wan, et al., PPAR-γ signaling in nonalcoholic fatty liver disease: pathogenesis and therapeutic targets, Pharmacol. Ther. 245 (2023) 108391. https://doi.org/10.1016/j.pharmthera.2023.108391.

[44] S. Almahmoud, H.A. Zhong, Molecular modeling of allosteric site of isoform-specific inhibition of the peroxisome proliferator-activated receptor PPARγ, Biomolecules 12 (2022) 1614. https://doi.org/10.3390/biom12111614.

[45] N. Zhang, F. Wei, S. Ning, et al., PPARγ agonist rosiglitazone and antagonist GW9662: antihypertensive effects on chronic intermittent hypoxia-induced hypertension in rats, J. Cardiovasc. Transl. Res. (2024) 1-13. https://doi.org/10.1007/s12265-024-10499-6.